



**Cathodic Protection Simulation of Linear Anode alongside  
Coated and Uncoated Pipe**

Journal:	<i>CORROSION</i>
Manuscript ID	CJ-1909-OA-3377.R3
Manuscript Type:	Original Article
Date Submitted by the Author:	n/a
Complete List of Authors:	Attarchi, Mehdi; Politecnico di Milano, CHIMICA, MATERIALI E INGEGNERIA CHIMICA "GIULIO NATTA" Ormellese, Marco; Politecnico di Milano, Chemistry, Materials and Chemical Engineering Brenna, Andrea; Politecnico di Milano, Chimica, Materiali e Ingegneria Chimica "G. Natta"
Key Words:	cathodic protection, metal pipes, polarization

# Cathodic Protection Simulation of Linear Anode alongside Coated and Uncoated Pipe

Mehdi Attarchi,\* Marco Ormellese,\*\* and Andrea Brenna\*\*\*

Dipartimento di Chimica, Materiali e Ingegneria Chimica "G. Natta", Politecnico di Milano.

## ARTICLE INFO

### Article history:

Received Day Month Year  
Accepted Day Month Year  
Available Day Month Year

### Keywords:

Cathodic protection, simulation, FEM, linear anode, coated pipe, uncoated pipe

\* Dipartimento di Chimica, Materiali e Ingegneria Chimica "G. Natta", Politecnico di Milano, Via Luigi Mancinelli 7, Milan, Lombardia, 20131, Italy.

Corresponding author: mehdi.attarchi@polimi.it

\*\* Dipartimento di Chimica, Materiali e Ingegneria Chimica "G. Natta", Politecnico di Milano, Via Luigi Mancinelli 7, Milan, Lombardia, 20131, Italy. (marco.ormellese@polimi.it).

\*\*\* Dipartimento di Chimica, Materiali e Ingegneria Chimica "G. Natta", Politecnico di Milano, Via Luigi Mancinelli 7, Milan, Lombardia, 20131, Italy. (andrea.brenna@polimi.it).

## ABSTRACT

Linear anode-pipe arrangement cathodic protection system with a complete nonlinear cathode boundary condition is analyzed by FEM numerical simulation to extract the effective parameters for both coated and uncoated pipe. The results show that defect size ratio, linear anode-to-pipe distance and pipe diameter are fundamental parameters to design an effective cathodic protection system able to guarantee a proper current distribution. Soil resistivity has a significant effect on the current distribution of both coated and uncoated pipe. The results show that the 100 mV potential shift criterion for a single linear anode-pipe arrangement can be ineffective and a two anode system may be required.

## INTRODUCTION

Cathodic protection (CP) is a useful industrial method to prevent corrosion of metallic structures exposed to conductive environments, such as soil and waters. This technique utilizes the circulation of direct current from an anode to the structure to be protected, the cathode. The protection current in a CP system lowers the potential of the cathode and its corrosion rate<sup>1</sup>. The current circulation can be obtained by the use of galvanic anodes or by an impressed current cathodic protection (ICCP) system; the

latter is typically adopted in environments with medium-to-high resistivity, as soil.

The anode part that supplies the protection current system may have a different shape and arrangement concerning the protection surface<sup>2</sup>. Anode could be installed close to the metal structure or in a remote position, to optimize the potential distribution at the cathode surface. Technically, different types and shapes of the anodes are used in an ICCP system. Among these systems, the linear anode configuration has an economical and technical advantage for different applications, such as protection of tank bottom plate, buried vessels, and drums as in case of piping in a congested area, piping with an aged or weak coating and piping in frozen soil. Despite the high applicability of this anode for a variety of CP systems, there are few studies about the potential and current distribution produced by the linear anode<sup>3-5</sup>. Moreover, the presence of a polymeric coating on the structure used in combination with CP makes this analysis more complex<sup>3, 6-8</sup>.

Linear anodes, namely anodes with length much higher than the diameter, are typically installed alongside the pipe. The two main subcategories of the linear anode are (a) wire anode with or without high conductive backfill and (b) noncircular section anode with circular low conductive backfill.

The determination of the electrical field established by a linear anode can be obtained utilizing numerical simulation, which may also take into account the boundary condition at the cathodic surface, namely the relationship between local potential and current density. Simulations can be done with different methods such as the finite element method (FEM)<sup>9-11</sup> or boundary element method (BEM)<sup>12-14</sup> or a combination of them<sup>15</sup>. Despite the advantages and limitations of each method, the definition of the boundary condition for the cathode and the setting of the relevant environmental factors are critical points for all of them.

The relation between current density and potential (or overvoltages) define by Butler-Volmer equation<sup>1</sup>. In the Butler-Volmer equation both activation overvoltages, i.e., electrical charge transfer at the electrode, and concentration polarization are considered, as in aerated electrolyte (soil and waters), the role of oxygen, governed by its mass transfer from the bulk to the cathode, becomes crucial<sup>16-18</sup>.

According to the ISO 15589-1 standard, the protection potential for carbon steel structures in an aerated condition (and resistivity lower than 100  $\Omega$  m) is -0.85 V vs. Cu/CuSO<sub>4, sat.</sub> (CSE)<sup>19</sup>. To avoid an overprotection condition with the risk of hydrogen embrittlement and cathodic disbonding on coated structures, the polarized potential of the protected structure should not be higher than -1.20 V vs. CSE. In other words, the recommended potential interval for appropriate protection is in between -0.85 V and -1.20 V vs. CSE. It follows that the protection polarized potential interval is  $\Delta\phi = 0.35$  V<sup>5, 6</sup>. In a conservative approach, this protection potential gap could be considered as 0.25 V, provided the -0.85 V vs. CSE criterion is guaranteed on all the structure surface. Another criteria for cathodic protection of the carbon steel in the condition mentioned above is a minimum cathodic potential shift of 100 mV from the OFF potential in a depolarization period of time, or 100 mV polarization from the structure native potential. This criterion is known as the 100 mV polarization shift. Nevertheless, based on the ISO standard, the application of the 100 mV potential shift should be avoided at operating temperatures above 40°C, in SRB-containing soils, when interference or external currents different from the protection one might be present. For the 100 mV polarization shift criterion, 0.05 V could be the maximum potential band for the most and least polarized part of the cathode surface. To sum up, 0.25 V or 0.05 V potential band could be used as a maximum allowable potential difference on the different part of the protected pipe. In NACE SP-

0169 both discussed criteria for carbon steel in soil,  $-0.85$  V vs. CSE and 100 mV polarization shift, are mentioned with little different approach<sup>20</sup>.

In the linear anode-pipe arrangement (Figure 1), an anode is placed parallel to the pipe. Under CP, the electric current path to the closest part of the pipe surface is shorter, so that part of the pipe could be more polarized. On the contrary, the remotest part of the pipe could be less polarized. For reaching complete protection, the potential of the closest and remotest part of the pipe shall be in a protection band. The use of structure-to-electrolyte potential is a fundamental method to assess CP level; by using the protection potential band (0.25 V) in comparing simulation data, upper and lower levels of polarization are simplified, without considering free corrosion potential.

## MATERIALS AND METHODS

### Simulation Model

The linear anode typically installs alongside and parallel to a pipe in the same or similar sandfill and backfill of pipe and close to it. From the numerical simulation point of view, two cases are considered:

Case a) Coated pipe with high resistance coating and some defects. Different possible situations could be assumed; for simplification and understanding, two opposite circular defects in the coating are considered at two extreme locations, remotest and nearest point with respect the linear anode, as presented in Figure 1. These two defects, close and remote, absorbed all protection current. The only exception for the cathode site is the section about defect location. In this case, the coated pipe with two defects, a 3D model has been implemented;

Case b) Pipe without coating or with an aged or weak coating. Whole pipe surface absorbed protection current. In this case, the length of the pipe could be eliminated from the model, and a 2D simulation could be representative of the real condition.

In Figure 2, the typical graphical solutions for the current distribution of the two cases are present.

The assumed diameter of the anode is 3 mm, while increasing the effective anode diameter with circular cross-section backfill, does not affect the model. The center point of the anode cross-section is the center point of the current lines outward the anode.

Pipe diameter ( $D_p$ ) ranges from 0.25 m (10 in.) to 1 m (40 in.). Linear anode-pipe distance ( $r_a$ ) varies from 0.1 to 1 m. Soil resistivity ( $\rho$ ) changes from 10  $\Omega$  m, water-saturated soil, to 5000  $\Omega$  m, desert, and frozen soil<sup>21</sup>. The close defect diameter ( $D_c$ ) and the remote defect diameter ( $D_R$ ) varies from 0.1 to 10 cm. The large defect diameter could be representative of a coating disbonding.

The dimension of the simulation field is 10×10 m, and for case a), 5 m length of pipe and anode is considered in the model. The mesh dimensions changes from 0.012 cm to 6 cm. The simulation results are superimposed on the boundary condition to check the validity of the model. Moreover, the total current of the anode and cathode compared with 0.1% error acceptance range<sup>22</sup>.

### Variables and Boundary Conditions

In case b (pipe without coating) linear anode-pipe distance ( $r_a$ ), pipe diameter ( $D_p$ ), soil resistivity ( $\rho$ ), linear current output ( $I$ ) and polarization behavior of the pipe are the variables. In case a (coated pipe), also the diameter of the defects, the defects size ratio and the position of the defect are variables, too.

The anode supply a constant current in the range of 1000 mA.

At the cathodic surface, i.e. the pipe, the relationship between local current density and potential follows the Butler-Volmer equation:

$$i = i_{\text{corr}} \cdot e^{((2.3(\phi - \phi_{\text{corr}}))/\beta_{\text{Fe}})} - i_{0,\text{H}_2} \cdot e^{((-2.3(\phi - \phi_{\text{H}_2}))/\beta_{\text{H}_2})} \quad (1)$$

Table 1 summarizes the values of the parameters used to define the boundary conditions at the cathodic surface. Values have been defined based on field and literature data, as described in a previous paper<sup>22</sup>. The selected boundary conditions present in Figure 3. The difference between boundary condition 1 (B.C. 1) and boundary condition 2 (B.C. 2) is the limiting diffusion current density of oxygen reduction reaction (ORR) that changes from 20 to 2 mA/m<sup>2</sup>, respectively.

In the present study FEM boundary condition are assumed to be constant in time, so polarization and FEM analysis results are in stable condition.

## RESULTS

In the presence of an ideal condition where a coated pipe has just one defect, the polarized potential of the defect could be easily measured. The complexity arises when two or more defects are present on the two opposite sides of the pipe. In this arrangement, the two defects show a different level of polarization. This arrangement, two defects in the opposite side, Figure 1, creates maximum competition in polarization, so it could be considered an extreme case.

More than 800 simulations are carried out for extracting the graphs hereafter presented. The potential profile, current density, maximum, and minimum values are extracted. A potential profile for two cases is presented in Figure 4. For case b), in the part of the coated surface, electrolyte potential is presented with a dotted line. For case a), potential of the center point of defects are considered as a potential of each defect in different conditions. For case b), the potential profile continues, and the remotest and the closest point will polarize most and least in each condition, respectively.

After validating data mentioned in section Materials and Methods, the effect of different variables are extracted and mentioned in this section. The variables are size and ratio of defects, location of defects, soil resistivity, anode current output, pipe diameter, and linear anode-pipe distance.

### Defect Size Ratio

Figure 5 shows the potential of the remote and close defect and the potential difference between remote and close defects as a function of the cathodic current density, derived from the simulation performed in the following condition: pipe diameter 0.4 m, linear anode-pipe distance 0.4 m, soil resistivity 100  $\Omega$  m. Three defect size ratio that defined as  $D_R/D_C$  has been considered: 1, 2, and 10. In all the ratio of Figure 5, the biggest defect is the most remote one.

In the presence of two similar defects (ratio equal to 1), the potential difference is almost negligible, i.e., the two defects have the same level of polarization. In addition to Figure 5, other simulations for ratio one between defect sizes,  $D_R/D_C$ , shows the negligible potential difference between both sides for defects diameter from 0.1 to 10 cm.

With increasing defect size ratio, the potential difference increases in the same current output of anode. The relation between size ratio and potential changes is nonlinear because of the nonlinear boundary condition. The polarization potential profile of the defects with different size is quite similar to the defined boundary condition graph that shifted in each condition. The value of the potential difference even in extreme case (ratio 10, highest cathodic current

density) is lower than 0.25 V, even if it is higher than 0.05 V. From the potential profile extracted from the simulation, the protection level at the remotest defect is about -0.85 V CSE; accordingly, the potential of the defect at closest point is never in overprotection condition. For high defect ratio, i.e. 10 here, if the measured potential of the pipe, which is a value between the potential of the remote and close defect, becomes close to the over-protection potential limit, there is a chance to unexpected over-protection (Figure 5c).

The 100 mV polarization shift potential is applicable where a high polarization is not attainable or suitable, so the applied current is close to the required protection current density. In Figures 5a to 5c the polarization curves around the protection current are overlapped, so the potential difference, shown in Figure 5.d, could be used for this purpose. Potential band higher than 0.05 V make it clear that from the 100 mV polarization shift criteria point of view, even with current density in the protection range such as current density around 20 mA/m<sup>2</sup> of Figure 5, it is not possible to conclude that the entire surface is sufficiently polarized, minimum 100 mV. In the second case, minimum 100 mV polarization shift in whole cathode sites could be guaranteed when the total polarization is much higher than 100 mV and requires a more detailed investigation for each case.

### Defect Location

In this section, four possible defect arrangements, different from Figure 1, are used to understand the effect of defect location. In all four arrangements, the diameter of the small defect is 1 cm, and the diameter of the large defect is 10 cm. The four arrangements are:

Arrangement 1: Small defect is close to the anode, and a large defect is on the opposite side

Arrangement 2: Opposite of Arrangement 1, large defect is close to the anode, and a small defect is on the opposite side

Arrangement 3: Small defect at the top of the pipe and large defect in the bottom side of the pipe

Arrangement 4: Small defect is close to the anode, and a large defect is on the top of the pipe

In the wide range of the anode current output, the potential difference of two defects for the four mentioned arrangements in soil with 100 Ω m resistivity is presented in Figure 6. Based on the boundary condition 1, protection current density is 20 mA/m<sup>2</sup>, so for two defects of Figure 6 with 1 and 10 cm diameter, protection current would be 0.16 mA. Moreover, the absolute value of the local potential shows that in the present condition and boundary condition, in current output higher than 0.6 mA, all the cathode surfaces are in the overprotection. These two lines are vertically shown in Figure 6b and c.

Location of the small and large defect in arrangement 1 and 2 is exactly the opposite. The graph of potential differences of two cases, graph (a) of Figure 6, is mirror-like, meaning that the location of the defects is not essential when both are in opposite sides.

Other arrangement and considering the top, bottom, and side locations for defects are presented in Figure 6 (b). In the protection current range, the different arrangement of defect shows a similar potential difference of two cathodes. In the high current output of anode, arrangement 1, which is one defect in front of the anode and another defect in the opposite side, in comparison with other cases, shows the maximum potential changes.

### Soil Resistivity

Soil resistivity, related to soil water retention, has a fundamental impact on the electrical field established by a CP system, and consequently, on the potential distribution by the cathodic current. In a specific condition, i.e. boundary condition B.C. 1,  $D_p = 0.4$  m,  $r_a = 0.4$  m and  $I_{anode} = 0.16$  A, which is equal to 20.2 mA/m<sup>2</sup> current density at cathode surface, effect of soil resistivity ranging from 10 to 5000 Ω m is illustrated in Figure 7. In the real field, increasing soil resistivity could happen when it is drought or frozen, and decreasing could happen when the water content of the soil is increased<sup>23</sup>.

Increasing soil resistivity will increase the potential gap between the two defects. The potential gap in high resistivity soil can shift the potentials to the range of "no protection" and "over protection".

### Soil Resistivity and Anode Current Output

As illustrated in Figure 7, increasing the soil resistivity could increase the potential difference at the two defects. The effect of soil resistivity could be combined with current output, which is a variable parameter in the hand of cathodic protection engineers. The increasing of the anode output will reduce the potential at the cathode, but with different level (Figure 8). In the low current output range, both close and remote defects receive a low amount of current and the polarization level is low. In the medium current range, when the potential at the cathode surface is in the region of diffusion control of oxygen reduction reaction (ORR), small changes in current density could change the potential sharply. In the high current region, above protection current, both defects reaches the hydrogen evolution reaction (HER) potential range, and the potential difference is reduced, due to Tafel slope of the hydrogen evolution reaction and accordingly to the high current needed to change potential in the HER region.

The combined effect of soil resistivity and anode output is presented in Figure 9 for  $D_p = 0.4$  m,  $r_a = 0.4$  m,  $D_c = 1$  cm,  $D_R = 10$  cm and boundary condition B.C. 1. Corrosion protection could not be achieved in potential range more positive than -0.85 V vs. CSE in Figure 9a-c and current output lower than protection current in Figure 9d ("no protection" area). As presented in Figure 9a-c, increasing soil resistivity will increase the gap between the polarization graphs of two defects. Moreover, increasing soil resistivity sharpened the potential profile changes of the close defect that has a small diameter, 1 cm, in the current density around the protection current. This change leads to intensifying the potential difference between two sides and the chance of over-protection in the small defects and no protection in the big defect, especially around the protection current.

Figure 9d shows that the gradual increasing potential difference pattern as a function of anode current output, changes in high resistivity soil. In a high resistivity soil ( $\rho \geq 200$  Ω m), a potential difference peak will appear corresponding to the protection current. The peak of Figure 9 shows that the in high resistivity soil, the potential difference will intensify to values more than acceptable range (0.25 V). While, in low resistance soil,  $\rho < 200$  Ω m, the potential difference is higher than 0.05 V and lower than 0.25 V, especially around the protection current. When the potential band is higher than 0.05 V, because of sharp changes in the polarization of the two defects in comparison with each other, it is not possible to be sure with 100 mV polarization criteria at current density close to the protection current, and meet the standard criteria<sup>20</sup>. This condition is in comply with the Figure 7, too.

Beside soil resistivity, oxygen diffusion is a critical parameter<sup>18</sup>, because changing in the diffusion of oxygen, as presented in Figure 3 and Table 1, could change the corrosion rate. Lower oxygen diffusion rate when other parameters are constant means lower corrosion rate. Figure 10 shows the potential difference of two proposed cathodes on the pipe surface as a function of anode current output. Three conditions are compared: soil resistivity 500 Ω

m and protection current density 20 mA/m<sup>2</sup> (B.C. 1); soil resistivity 500 Ω m and protection current density 2 mA/m<sup>2</sup> (B.C. 2); extreme soil resistivity 5000 Ω m and protection current density 2 mA/m<sup>2</sup> (B.C. 2); in Figure 10a to c, respectively.

In high soil resistivity,  $\rho = 500 \Omega \text{ m}$  here, the potential difference shows a maximum peak (at 0.2 A anodic current) higher than the acceptable range of protection criteria. This maximum will disappear in the same soil resistivity and low aerated soil (B.C.2). A similar peak to the first condition,  $\rho = 500 \Omega \text{ m}$  and B.C. 1, is present if extremely high resistivity soil is considered,  $\rho = 5000 \Omega \text{ m}$ , in the case of a low limiting current density (B.C. 2).

The potential difference shows a peak when the protection current is applied. This condition is similar to the medium current of Figure 8. In this condition, absorbed current in two cathodes are similar, but the potentials are different. From an electrical analysis point of view, in a constant current, high potential difference means a high resistance between these two points. This resistance leads to a voltage drop between these two cathodes. Similar potential differences, two peaks of Figure 10d, for soil with  $\rho = 500 \Omega \text{ m}$  and 20 mA/m<sup>2</sup> limiting current density or  $\rho = 5000 \Omega \text{ m}$  and 2 mA/m<sup>2</sup> limiting current density means similar voltage drop is required to make a maximum difference in polarization level at two defects at two extreme locations.

In both boundary conditions, a maximum potential difference appears in the protection current, but in the sufficiently high soil resistance. Moreover, the potential difference in most cases could not meet the 0.05 V potential band criteria and there is a possibility of insufficient protection or over-protection for current close to protection current.

Analysis of the effect of current density and soil resistivity for case b), which is representative of weak coated pipe or bare surface, is presented in Figure 11. For better comparison, the similar condition of Figure 10 is used ( $D_p = 0.4 \text{ m}$ ,  $r_a = 0.4 \text{ m}$  and B.C. 1). In comparison with the case a), depicted in Figure 9, the effect of soil resistivity in intensifying the potential difference is more evident in case b), where the whole surface of the pipe could absorb current (Figure 11). In case b) and B.C. 1, as presented in Figure 11, in soil with a resistivity between 200-500 Ω m, the potential difference peak will be broadened for the quite wide range of current output (20-50 mA). Comparing Figure 9 and Figure 11, in the same physical condition ( $D_p = 0.4 \text{ m}$ ,  $r_a = 0.4 \text{ m}$  and B.C. 1) the maximum potential difference is increased from 0.35 V in case a) to 0.65 V in case b). In case b) and high soil resistivity the polarization graph of the two defects shows a really different behavior (Figure 11b) which is the source of high broadened potential difference peak (Figure 11c.) The potential difference for case b) in soil resistivity equal or higher than 100 Ω m is much higher than the acceptable potential band of both mentioned criteria, 0.25 V and 0.05 V. In this condition, case b) with high resistivity soil and high protection current density (B.C.1), Figure 11b, a linear anode could not supply a suitable current distribution at the pipe surface. Effective parameters for reducing the potential difference will be discussed in further sections.

In the case b), decreasing protection current density from 20 to 2 mA/m<sup>2</sup> will reduce the maximum possible potential difference, as presented in Figure 12. Moreover, an increase of one order of magnitude in soil resistivity, similar to case a) depicted in Figure 10, could not compensate the voltage drop that needs for maximizing potential differences. While, similar to case a), a maximum potential difference appears in protection current. The absolute value of the potential difference for case b) with one order of magnitude reduction in limiting current density could reduce the potential difference,  $\Delta\phi$ , to the acceptable range of potential band of protection criteria. It means, for high resistivity soil, when bedding of the pipe is excellent and the soil is sufficiently compact, a significant

reduction in limiting current density is assured; a linear anode could be used for protection of poor coating or bare pipe. However, for poor coated pipe (Figures 12a), the limiting current density is high; a linear anode should not be used in this case because even the potential profile at the pipe surface is not attainable. In the real measurement, the potential is in between the values of the closest and remotest defects, but in the mentioned case, potentials are in no protection area or over-protection range, both not desirable protection ranges.

As presented in Figure 11 and Figure 12 in the extreme cases and highest soil resistivity the potential difference for bare pipe could reach to the range of 0.6 V. This maximum is equal to the range of potential that oxygen reduction reaction (ORR) predominate. Another possibility to see the maximum potential changes for a coated pipe similar to the bare pipe is a big difference in defect size. For example, increase defect diameter size ratio from 0.01 m/0.1 m to 0.001 m/0.1 m, and in 500 Ω m soil resistivity, the maximum potential difference for coated pipe reaches to 0.42 V.

### Pipe Diameter

Figure 13 reports results of simulations performed varying the pipe diameter of case a) from 0.25 m to 1.0 m in the following conditions:  $r_a = 0.4 \text{ m}$ ,  $\rho = 100 \Omega \text{ m}$ ,  $D_c = 1 \text{ cm}$ ,  $D_R = 10 \text{ cm}$ , protection current density 20 mA/m<sup>2</sup> (B.C. 1). The greater the pipe diameter, greater the distance between the two defects absorbing current. Nevertheless, the effect of pipe diameter on the potential difference of two defects is negligible: the absolute value of the potential difference is not changed too much, so if a linear anode-pipe system in a specific defect ratio and soil resistivity is in the adequate potential protection range like 0.25 V, changing the pipe diameter could not increase it to out of range or vice versa.

The potential difference of two sides for the similar condition of Figure 13 for case b) is presented in Figure 14. The profile of potential changes in increasing  $D_p$  is quite similar to the effect of soil resistivity (Figure 11). The maximum potential difference of two sides of the bare pipe is quite close to the potential range that ORR diffusion polarization is dominant.

### Linear Anode-Pipe Distance

Linear anode-pipe distance,  $r_a$ , is a big challenge in practice. In comparing all the above parameters, this distance is selected by cathodic protection designer. The simulation results for the coated pipe show that  $r_a$  has a negligible effect on the level of polarization of two defects at two sides, in the typical range of physical parameters. This effect is repeated even in high resistivity soil, such as 500 Ω m, which shows a peak in potential difference versus applied current (Figure 15). On the other hand, it means that increasing linear-anode-pipe distance could not reduce significantly the potential differences on the proposed cathode at two sides of the coated pipe.

The effect of linear anode-pipe distance for case b) is illustrated in Figure 16 ( $D_p = 0.4 \text{ m}$ ,  $D_c = 1 \text{ cm}$ , and  $D_R = 10 \text{ cm}$  and B.C. 1). The entire pipe surface is absorbing the protection current, and  $r_a$  is highly affecting the potential distribution on the pipe. Moreover, this effect is magnified by the resistivity. Comparing the absolute value of potential differences for the two cases (Figure 15 and Figure 16), the coated pipe with defect could be well polarized in the acceptable range, while in the presence of a weak coating or a bare pipe (case b) to meet the criteria the distance should be increased even more than 2-3 times of pipe diameter. Although some successful filed experiences show that fixed linear anode-pipe distance, e.g. 25 or 80 cm, could guarantee sufficient protection, even in different soil resistivity.

For the bare pipe (case b) the only practical variables to bring the potential band into the acceptable range is the linear anode-pipe distance. This variable is effective, especially for low resistivity soil. For example, as presented in Figure 16, increasing distance to 1 m for  $D_p = 0.4$  m and soil with resistivity around  $100 \Omega \text{ m}$  could reduce the potential gap to lower than 0.25 V. However, for bare pipe, for the wide range of soil resistivity and  $r_a$ , the potential gap in the current around protection current could not reach to 0.05 V band requirement.

## DISCUSSION

Effect of different parameters and scenarios are studied in the results section. These results could be roughly estimated and analyzed by primary current distribution, where just electrical ohmic laws are valid. Another effective parameter is electrochemical behavior of the cathode at the soil interface, which is known as secondary current distribution.

A schematic current path with the proposed resistance for both cases a) and b) is presented in Figure 17:  $R_{S1}$  is soil resistance between anode and closest point of the pipe;  $R_{Sn}$  is resistance of soil close to the pipe;  $R_{P1}$  and  $R_{P2}$  are resistance of the cathode defects;  $R_{Pn}$  represents the resistance of the whole pipe surface.

Based on Ohm's law, the current will flow more through the less resistive path. In case a), there are only two cathodes and just two  $R_{Sn}$  is in between, so the competition is just between two paths. However, when the pipe surface is bare, the whole surface of the pipe is able to absorb the protection current. In a simplified model the pipe surface could be transferred to the limited number of elements, so each element of the pipe surface in case b) could absorb the current. On the other hand, from the nearest point to the linear anode to the remotest point, the current has access to the cathode surface to return to the protection circuit. So, around the pipe, a different current path is available with a gradual increase in resistance.

Based on the electrical scheme depicted in Figure 17 (case a), in a simplified approach, the primary current distribution could be used for a rough estimation of the effect of different parameters such as  $D_p$ ,  $r_a$ , and  $\rho$ . In the analysis that presents for some cases in Table 2, the resistance of circle cathode defect,  $R_{P1}$ , and  $R_{P2}$ , is calculated from  $R = \rho/2 \cdot D_{def}$ . Soil resistance between two points could be calculated from  $R = \rho/d$  equation for  $R_{S1}$  and  $R_{Sn}$ . In both equations,  $\rho$  is soil resistivity ( $\Omega \text{ m}$ ),  $D_{def}$  is the diameter of the defect (m) and  $d$  (m) is the distance of two points in the space. Secondary current distribution elements are hidden in the  $R_p$  of the Figure 17 model. The related resistance values of the secondary current distribution are hard to calculate directly, and this is the main reason that simulation can give a more realistic value than primary current distribution analysis<sup>22</sup>.

Based on the data depicted in Figure 5, defect size ratio is an effective parameter in the potential difference of two defects, while as shown in Figure 6, the location of defects is not the determining parameter in potential difference. The extracted potential gap from simulation results for the typical range of defect size, diameter from 0.1 to 10 cm, could lead to a potential gap more than 0.05 V, so using 100 mV polarization criteria could be **an issue**.

As presented in Figure 7, increasing soil resistivity will increase the potential difference between the two defects. Based on Figure 8, the maximum potential difference of two sides occurs when diffusion polarization of ORR is predominant. In the diffusion part of the polarization curve, e.g., medium current of Figure 8, little changes of current could change the potential very rapidly, so from ohm principle ( $R = \Delta\phi/\Delta I$ ), the resistance of the surface tends to be very high value or infinity. If  $R_p$  (summation of primary and secondary

current distribution resistance part at cathode's surface) of Figure 17 (a) tend to very high values, other resistance parts become ineffective in determining the polarization level of each cathode. In this circumstance, the critical parameter is that one can control the current ratio between the two cathodes. Last two columns of Table 2 shows that defect resistance is the determining resistance in protection circuit resistance and so rate determines element in the amount of absorbed current at each cathode (Figure 17).

When the current density is increased to the protection range, and the  $R_p$  becomes a predominant element, other resistance parts become ineffective. The relation between resistance and the potential difference mentioned in Figure 7(b) is presented in Figure 18. The applied current value, 0.16 mA, is little above the protection current, and it is expected to shift the potential of the cathodes to the diffusion control part. Based on boundary condition, Figure 3, the potential range is about 0.4 V, from -0.6 to -1.0 V vs. CSE. So in the low resistivity environment, the absolute value of the cathodes potential are close to each other, Figure 7(a). In the range of diffusion polarization, where the secondary current distribution shows very high polarization resistance, the relation between soil resistivity and the potential difference is linear, Figure 18. If all the resistance of different part in Figure 17 remains comparable with polarization resistance under diffusion control, the effect of soil resistivity becomes nonlinear. This linearity is the confirmation of predomination of the secondary current distribution in the polarization of two cathodes under diffusion control. This analysis shows why linear current distribution analysis that considers just primary current distribution or only linear relation between potential and current could not predict potential distribution on a similar geometry realistically<sup>4,5</sup>. This analysis, linear relation between the potential difference of two cathodes and soil resistivity, is just valid where both parts are sufficiently polarized to the diffusion range. For higher and lower potential range, where some part is under activation polarization control or HER reaction control, this linear relation is not valid, as Figure 7(b) shows more complex relation than polarization under one type of polarization, such as diffusion.

In the current output close to the protection current or on the other hand, close to diffusion limiting current, increasing resistivity could increase the potential difference of two cathodes. This effect appears as a peak in Figure 9d and Figure 10d. For coated pipe with two defects, case a), in high resistance soil, which means more than  $200 \Omega \text{ m}$  here, the potential gap could decrease just in high current output of the anode. Otherwise, where the potential gap is more than 0.25 V, some part is out of protection. Figure 10 makes it clear, the maximum peak in the potential difference at protection current could be repeated in lower limiting current density, relative higher resistance soil ( $500 \Omega \text{ m}$  resistivity and  $2 \text{ mA/m}^2$  limiting current density here). As per the above analysis, this peak is a sign of sufficient voltage drop between two separate cathodes.

In a bare pipe or weak (aged) coated pipe, case b), the whole pipe surface could absorb current gradually, so just one separate cathode is not polarized, the cathode and other small cathodes in the vicinity of it could be polarized as well. In this case, if for example closest part of the pipe to the anode is polarized sufficiently, in the same time the area around of this small cathode could be polarized as well and streaming protection current, not willing to go to the other side of the pipe, where another cathode is available next to polarized cathode. For this reason, in the case of b), the current is absorbed, and the peak of the potential difference of two sides of the pipe broaden in Figure 11c. The continuous path of returning current to the protection circuit in case b), make a nonlinear relation between resistivity and potential difference even in the diffusion control part, so in comparison to Figure 10, in Figure 12 the maximum potential difference of two sides could not repeat, even in high resistivity soil. In the case of b), the absolute value of potential difference for a wide

range of current and soil resistivity is high and need more care for reducing the potential differences.

Based on Figure 13 and Figure 15, pipe diameter and linear anode-pipe distance have an insignificant effect on the potential difference in case a), coated pipe with two defects. The root of this effect comes from primary current distribution analysis. Primary current distribution analysis of item 1 and 2 in Table 2 shows one order of magnitude difference between the resistance element of the defect and soil. Therefore, the effect of  $D_p$  that is part of the soil resistance path in comparison with the whole resistance of the protection circuit for the presented range of data is insignificant. The analysis of Figure 15, comparison between item 1 with 3 and item 2 with 4 of Table 2, shows the effect of increasing the linear anode-pipe distance from 0.4 m to 1 m for two different pipe diameters, from primary current distribution analysis. In the simplified approach that presented in Table 2, the absolute value of the soil resistance,  $R_{s1}$ , and its changes from an increasing distance in comparison with defect-to-earth resistance is one order of magnitude lower. Therefore, based on primary current distribution analysis, it is reasonable that  $r_a$  is an insignificant parameter in the coated pipe, case a).

Effect of pipe diameter on the potential difference of two sides of the pipe in case b), bare pipe, is significant, Figure 14. Potential difference not only affected by the soil path, but also gradual current absorption will intensify it. The schematic of the current path is presented in Figure 17 (b). Increasing  $D_p$  means increasing the polarizable path for returning the current to the protection circuit. Moreover, as shown in Figure 16, linear anode-pipe distance has a significant effect on the potential difference of two sides. Comparing case a) and b), the maximum potential difference of two sides is high, but it can be reduced by an increasing distance between linear anode-pipe. When large diameter poorly coated or bare pipe exists, two linear anode maybe needed, one each side of the pipe.

## Conclusions

Main conclusions for linear anode-pipe arrangement in a typical range of variables are:

- ❖ In a coated pipe, defect size and location have an insignificant effect on the potential difference of them, but the size ratio of the defects is essential.
- ❖ Soil resistivity and limiting current density are effective parameters in the gradient of potential distribution on the surface of the pipe, in both coated and uncoated pipe. Proper compaction and bedding of soil around the pipe for reducing limiting current density is essential to have an excellent potential distribution at the pipe surface.
- ❖ Pipe diameter and linear anode-pipe distances are two effective parameters on the potential gradient at the pipe surface for bare pipe, not coated. The effectiveness of these parameters is profoundly affected by soil resistivity.
- ❖ The applicability of 100 mV potential decay for the linear anode-pipe arrangement, due to the wide range of variables, needs a further investigation.

## References

1. Lazzari, L., *Engineering Tools for Corrosion: Design and Diagnosis* (Duxford: WP, Woodhead Publishing, an imprint of Elsevier, 2017).
2. Baeckmann, W. von, W. Schwenk, and W. Prinz, eds., *Handbook of Cathodic Corrosion Protection: Theory and Practice of Electrochemical Protection Processes*, 3. ed (Houston, Tex: Gulf Publ. Co, 1997).

3. Kennelley, K.J., L. Bone, and M.E. Orazem, *CORROSION* 49 (1993): pp. 199–210.
4. Martinez, S., *Mater. Corros.* 61 (2010): pp. 338–342.
5. Newman, J., *J. Electrochem. Soc.* 138 (1991): p. 3554.
6. Orazem, M.E., K.J. Kennelley, and L. Bone, *CORROSION* 49 (1993): pp. 211–219.
7. Orazem, M.E., J.M. Esteban, K.J. Kennelley, and R.M. Degerstedt, *CORROSION* 53 (1997): pp. 427–436.
8. Orazem, M.E., J.M. Esteban, K.J. Kennelley, and R.M. Degerstedt, *CORROSION* 53 (1997): pp. 264–272.
9. Marcassoli, P., A. Bonetti, L. Lazzari, and M. Ormellese, *Mater. Corros.* 66 (2015): pp. 619–626.
10. Xu, L.Y., and Y.F. Cheng, *Corros. Sci.* 78 (2014): pp. 162–171.
11. Li, C., M. Du, J. Sun, Y. Li, and F. Liu, *J. Electrochem. Soc.* 160 (2013): pp. E99–E105.
12. Yan, J.-F., *J. Electrochem. Soc.* 139 (1992): p. 1932.
13. Zhao, L., X. Wei, G. Cui, and Z. Li, *Anti-Corros. Methods Mater.* 62 (2015): pp. 407–415.
14. Sun, W., and K.M. Liu, *J. Electrochem. Soc.* 147 (2000): p. 3687.
15. Brichau, F., and J. Deconinck, *CORROSION* 50 (1994): pp. 39–49.
16. Kodým, R., D. Šnita, V. Fíla, K. Bouzek, and M. Kouřil, *Corros. Sci.* 120 (2017): pp. 28–41.
17. Kodým, R., D. Šnita, V. Fíla, K. Bouzek, and M. Kouřil, *Corros. Sci.* 120 (2017): pp. 14–27.
18. Gadala, I.M., M. Abdel Wahab, and A. Alfantazi, *Mater. Des.* 97 (2016): pp. 287–299.
19. ISO 15589-1, "Petroleum, Petrochemical and Natural Gas Industries — Cathodic Protection of Pipeline Systems, Part 1: On-Land Pipelines" (ISO, 2015).
20. NACE SP-0169, "Control of External Corrosion on Underground for Submerged Metallic Piping Systems" (NACE, 2013).
21. Delaney, A.J., P.R. Peapples, and S.A. Arcone, *Cold Reg. Sci. Technol.* 32 (2001): pp. 107–119.
22. Attarchi, M., M. Ormellese, and A. Brenna, *CORROSION* 75 (2019): pp. 1128–1135.
23. Tagg, G.F., *Earth Resistances* (Pitman Publishing Corporation, 1964).

## FIGURE AND TABLE CAPTIONS

FIGURE 1. Schematic of the linear anode and pipe with two opposite defects.

FIGURE 2. Typical current distribution in 3D (case a) and 2D (case b) FEM simulation.

FIGURE 3. Graphical presentation of boundary conditions at the cathode.

FIGURE 4. Potential profile of pipe surface for both cases ( $D_p = 0.4$  m,  $r_a = 0.4$  m,  $\rho = 100$   $\Omega$  m, and B.C. 1, for case b  $D_R = 10$  cm and  $D_C = 5$  cm).

FIGURE 5. Effect of defect size ratio (a)  $D_R/D_C=1$ , (b)  $D_R/D_C=2$ , (c)  $D_R/D_C=10$ , and (d) potential difference for three cases ( $D_R = 10$  cm,  $D_p = 0.4$  m,  $r_a = 0.4$  m,  $\rho = 100$   $\Omega$  m, and B.C. 1).

FIGURE 6. Effect of defect location for  $\rho = 100$   $\Omega$  m,  $D_p = 0.4$  m,  $r_a = 0.4$  m, and Small Defect Diameter = 1 cm and Large Defect Diameter = 10 cm (a) Polarization defects ( $D_R = 10$  cm and  $D_C = 1$  cm) in arrangement 1, (b) comparison between potential difference of arrangement 1 and 2, (c) potential difference of arrangements 1, 3, and 4 (B.C. 1).

FIGURE 7. Effect of Soil Resistivity ( $D_p = 0.4$  m,  $r_a = 0.4$  m,  $D_C = 1$  cm,  $D_R = 10$  cm,  $I_{anode}=0.16$  A and B.C. 1).

FIGURE 8. Polarization of two points of pipe in different level of applied current.

FIGURE 9. Soil resistivity effect in case a (a)  $\rho = 10$   $\Omega$  m, (b)  $\rho = 100$   $\Omega$  m, (c)  $\rho = 200$   $\Omega$  m, and (d) potential difference for presented soil resistivity ( $D_p = 0.4$  m,  $r_a = 0.4$  m,  $D_C = 1$  cm,  $D_R = 10$  cm and B.C. 1).

FIGURE 10. Soil resistivity and limiting current density effect in case a (a) B.C. 1 and  $\rho = 500$   $\Omega$  m, (b) B.C. 2 and  $\rho = 500$   $\Omega$  m, (c) B.C. 2 and  $\rho = 5000$   $\Omega$  m (d) potential difference for three mentioned conditions ( $D_p=0.4$  m,  $r_a=0.4$  m,  $D_C=1$  cm,  $D_R=10$  cm).

FIGURE 11. Soil resistivity effect in case b (a)  $\rho = 10$   $\Omega$  m, (b)  $\rho = 500$   $\Omega$  m, and (c) potential difference for mentioned soil resistivity ( $D_p = 0.4$  m,  $r_a = 0.4$  m and B.C. 1).

FIGURE 12. Soil resistivity and limiting current density effect in case b (a) B.C. 1 and  $\rho = 500$   $\Omega$  m, (b) B.C. 2 and  $\rho = 500$   $\Omega$  m, (c) B.C. 2 and  $\rho = 5000$   $\Omega$  m (d) potential difference for three mentioned conditions ( $D_p = 0.4$  m,  $r_a = 0.4$  m and B.C. 1 and 2).

FIGURE 13. Effect of pipe diameter in case a (a)  $D_p = 0.25$  m, and (b) potential difference for mentioned pipe diameter ( $r_a = 0.4$  m,  $\rho = 100$   $\Omega$  m,  $D_C=1$  cm,  $D_R= 10$  cm and B.C. 1).

FIGURE 14. Effect of pipe diameter in case b (a)  $D_p = 0.25$  m, (b)  $D_p = 1.00$  m, and (c) potential difference for mentioned pipe diameter ( $r_a = 0.4$  m,  $\rho = 100$   $\Omega$  m and B.C. 1).

FIGURE 15. Linear anode-pipe distance in case a (a)  $r_a = 0.1$  and  $\rho = 100$   $\Omega$  m, (b)  $r_a = 0.1$  and  $\rho = 500$   $\Omega$  m, and (c) potential difference for two resistivity with different anode-pipe distance ( $D_p = 0.4$  m,  $D_C = 1$  cm and  $D_R = 10$  cm and B.C. 1).

FIGURE 16. Linear anode-pipe distance in case b,  $D_p = 0.4$  m and B.C. 1 for (a)  $r_a = 1.0$  and  $\rho = 100$   $\Omega$  m, (b) potential difference for  $\rho = 100$   $\Omega$  m and different anode-pipe distance, (c)  $r_a = 1.0$  and  $\rho = 500$   $\Omega$  m, and (d) potential difference for  $\rho = 500$   $\Omega$  m and different anode-pipe distance, (c).

FIGURE 17. Schematic of current paths and proposed resistance for the (a) case a and (b) case b.

FIGURE 18. Effect of soil resistivity for limited range ( $D_p = 0.4$  m,  $r_a = 0.4$  m,  $D_C = 1$  cm,  $D_R = 10$  cm,  $I_{anode}=0.16$  A and B.C. 1).

TABLE 1. Boundary conditions of the cathode.

TABLE 2. Primary current distribution analysis of case a with  $\rho = 100$   $\Omega$  m,  $D_C=1$  cm, and  $D_R= 10$  cm.



1  
2  
3  
4  
5  
6  
7  
8  
9  
10  
11  
12  
13  
14  
15  
16  
17  
18  
19  
20  
21  
22  
23  
24  
25

**Tables**

TABLE 1.

Parameter	Description	Qty. (B.C. 1)	Qty. (B.C. 2)
$\beta_{Fe}$	Anodic Tafel's slope	60 mV/decade	60 mV/decade
$i_{corr}$	Corrosion current density	20 mA/m <sup>2</sup>	2 mA/m <sup>2</sup>
$i_L$	ORR limiting current density	20 mA/m <sup>2</sup>	2 mA/m <sup>2</sup>
$\phi_{corr}$	Corrosion potential	-0.53 V vs. CSE	-0.58 V vs. CSE
$i_{0,H2}$	Hydrogen exchange current density on steel	0.01 mA/m <sup>2</sup>	0.01 mA/m <sup>2</sup>
$\beta_{H2}$	Hydrogen Tafel's slope	120 mV/decade	120 mV/decade
$\phi_{H2}$	Hydrogen eq. potential (pH = 8)	-0.472 V SHE -0.788 V CSE	-0.472 V SHE -0.788 V CSE

TABLE 2.

Item	$D_p$ (m)	$r_a$ (m)	$R_{S1}$ ( $\Omega$ )	$R_{S2}$ ( $\Omega$ )	$R_{P1}$ ( $\Omega$ )	$R_{P2}$ ( $\Omega$ )
1	0.25	0.4	250	400		
2	1	0.4	250	100	5000	500
3	0.25	1	100	400		
4	1	1	100	100		

26  
27  
28  
29  
30  
31  
32  
33  
34  
35  
36  
37  
38  
39  
40  
41  
42  
43  
44  
45  
46  
47  
48  
49  
50  
51  
52  
53  
54  
55  
56  
57  
58  
59  
60

1  
2  
3  
4  
5  
6  
7  
8  
9  
10  
11  
12  
13  
14  
15  
16  
17  
18  
19  
20  
21  
22  
23  
24  
25  
26  
27  
28  
29  
30  
31  
32  
33  
34  
35  
36  
37  
38  
39  
40  
41  
42  
43  
44  
45  
46  
47  
48  
49  
50  
51  
52  
53  
54  
55  
56  
57  
58  
59  
60

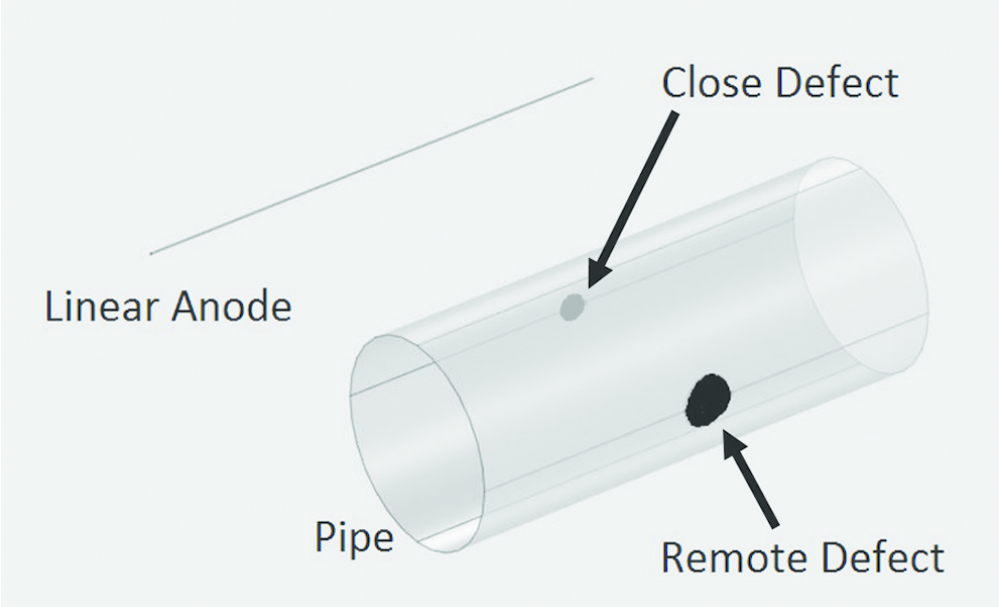


FIGURE 1. Schematic of the linear anode and pipe with two opposite defects.

83x50mm (300 x 300 DPI)

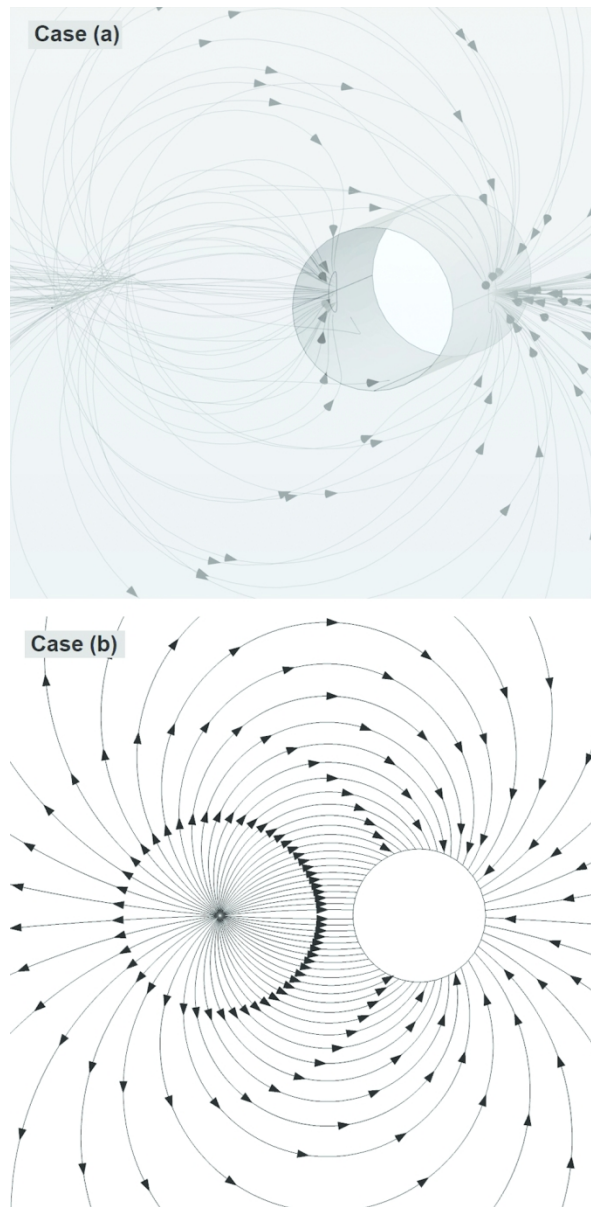


FIGURE 2. Typical current distribution in 3D (case a) and 2D (case b) FEM simulation.

83x170mm (300 x 300 DPI)

1  
2  
3  
4  
5  
6  
7  
8  
9  
10  
11  
12  
13  
14  
15  
16  
17  
18  
19  
20  
21  
22  
23  
24  
25  
26  
27  
28  
29  
30  
31  
32  
33  
34  
35  
36  
37  
38  
39  
40  
41  
42  
43  
44  
45  
46  
47  
48  
49  
50  
51  
52  
53  
54  
55  
56  
57  
58  
59  
60

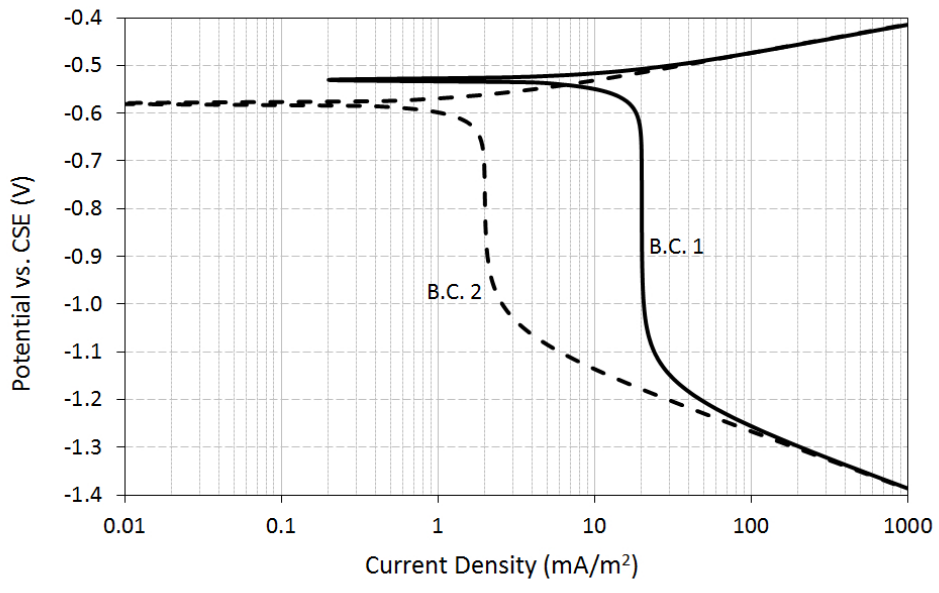


FIGURE 3. Graphical presentation of boundary conditions at the cathode.  
83x57mm (300 x 300 DPI)

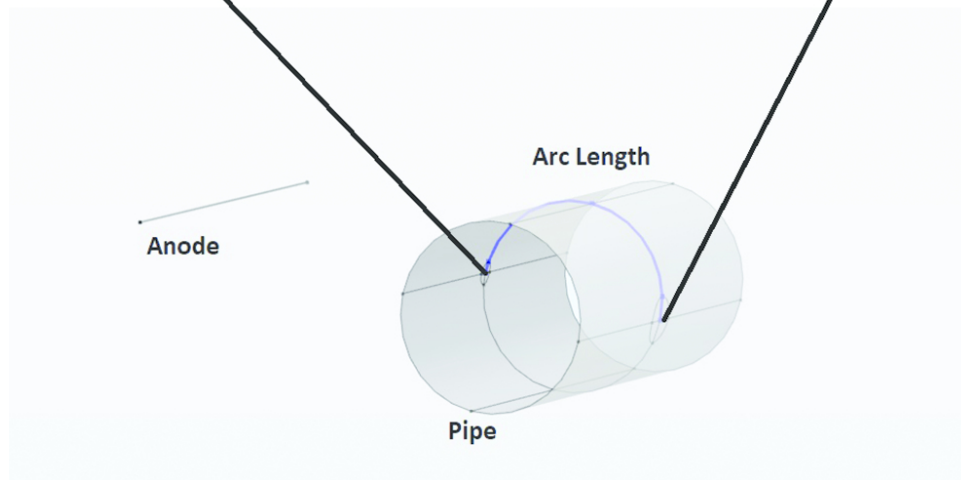
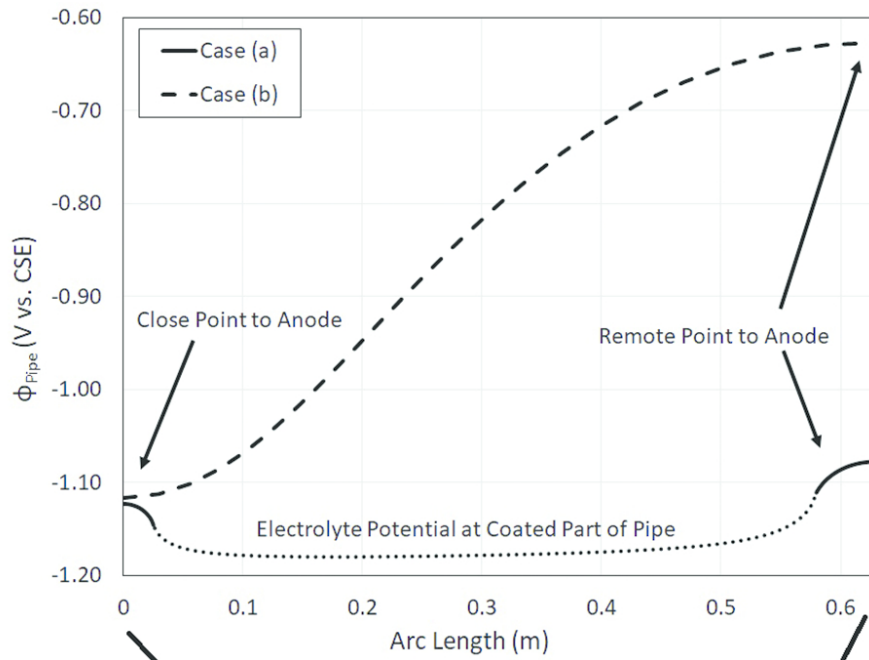


FIGURE 4. Potential profile of pipe surface for both cases ( $D_P = 0.4$  m,  $r_a = 0.4$  m,  $\rho = 100 \Omega$  m, and B.C. 1, for case b  $D_R = 10$  cm and  $D_C = 5$  cm).

83x104mm (300 x 300 DPI)

1  
2  
3  
4  
5  
6  
7  
8  
9  
10  
11  
12  
13  
14  
15  
16  
17  
18  
19  
20  
21  
22  
23  
24  
25  
26  
27  
28  
29  
30  
31  
32  
33  
34  
35  
36  
37  
38  
39  
40  
41  
42  
43  
44  
45  
46  
47  
48  
49  
50  
51  
52  
53  
54  
55  
56  
57  
58  
59  
60

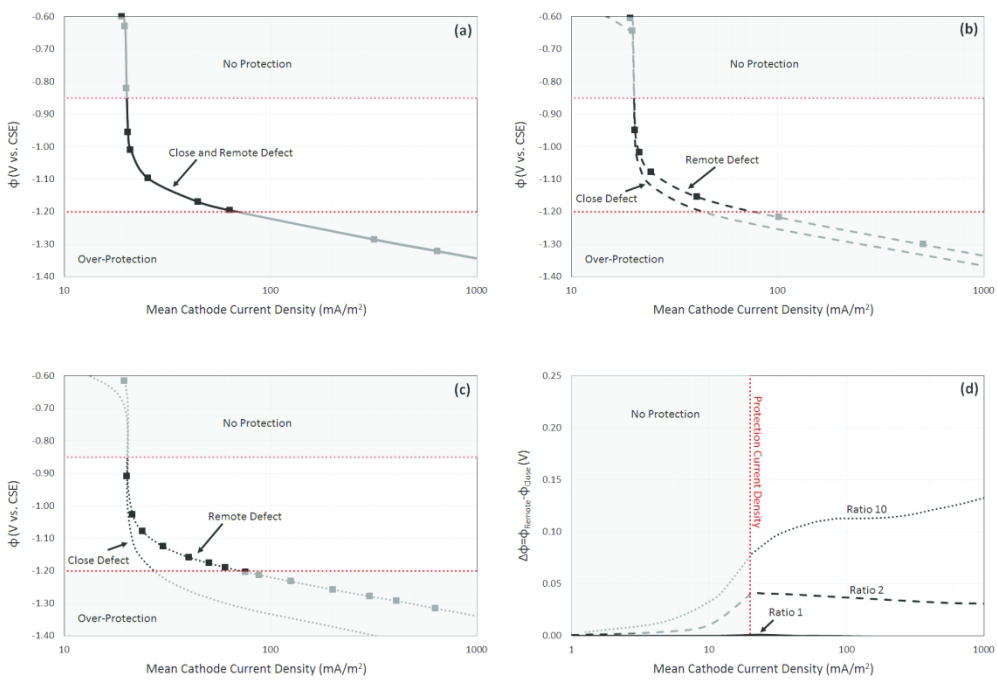


FIGURE 5. Effect of defect size ratio (a)  $D_R/D_C=1$ , (b)  $D_R/D_C=2$ , (c)  $D_R/D_C=10$ , and (d) potential difference for three cases ( $D_R = 10$  cm,  $D_P = 0.4$  m,  $r_a = 0.4$  m,  $\rho = 100 \Omega$  m, and B.C. 1).

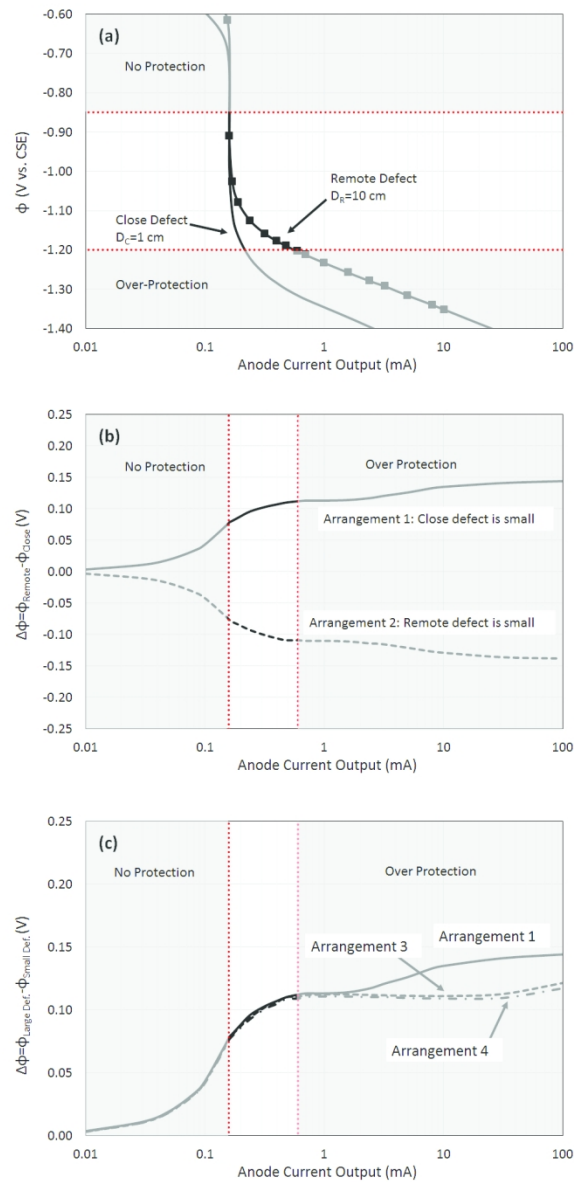


FIGURE 6. Effect of defect location for  $\rho = 100 \Omega \text{ m}$ ,  $D_P = 0.4 \text{ m}$ ,  $r_a = 0.4 \text{ m}$ , and Small Defect Diameter = 1 cm and Large Defect Diameter = 10 cm (a) Polarization defects ( $D_R = 10 \text{ cm}$  and  $D_C = 1 \text{ cm}$ ) in arrangement 1, (b) comparison between potential difference of arrangement 1 and 2, (c) potential difference of arrangements 1, 3, and 4 (B.C. 1).

1  
2  
3  
4  
5  
6  
7  
8  
9  
10  
11  
12  
13  
14  
15  
16  
17  
18  
19  
20  
21  
22  
23  
24  
25  
26  
27  
28  
29  
30  
31  
32  
33  
34  
35  
36  
37  
38  
39  
40  
41  
42  
43  
44  
45  
46  
47  
48  
49  
50  
51  
52  
53  
54  
55  
56  
57  
58  
59  
60

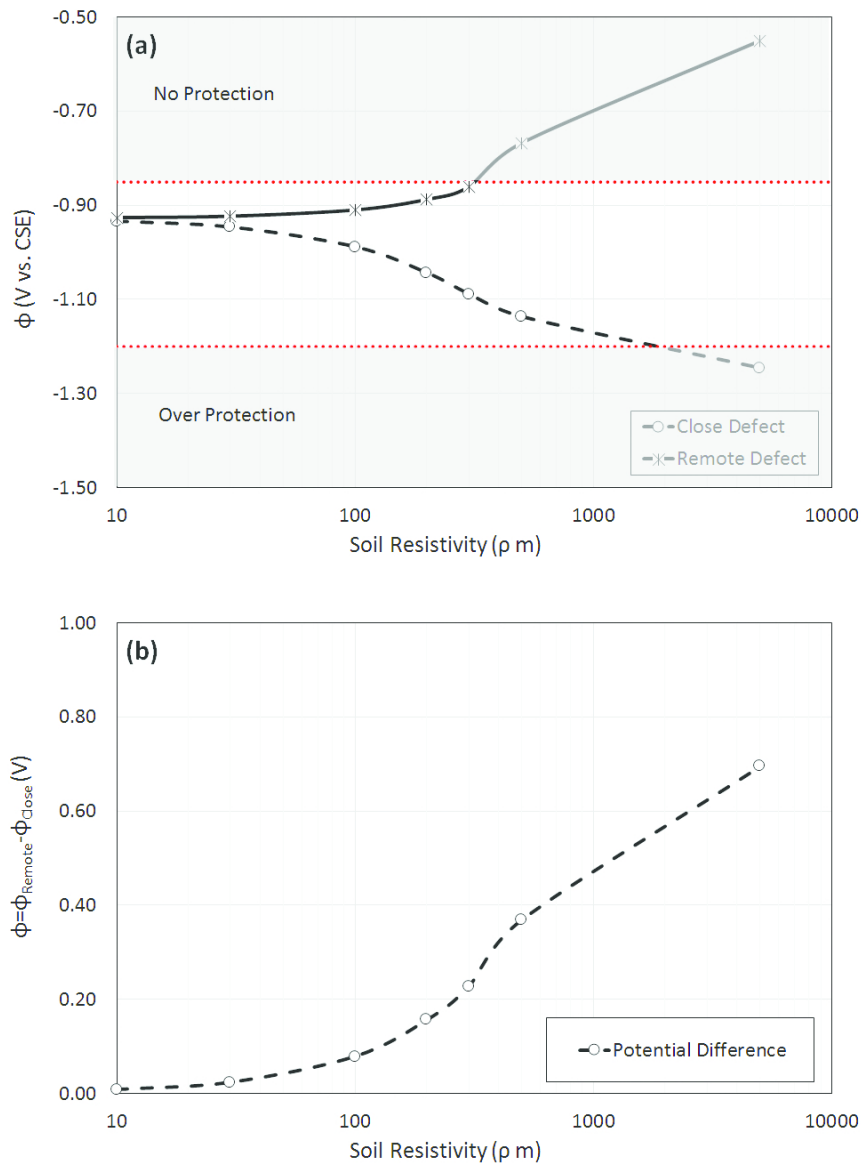


FIGURE 7. Effect of Soil Resistivity ( $D_p = 0.4 m$ ,  $r_a = 0.4 m$ ,  $D_C = 1 cm$ ,  $D_R = 10 cm$ ,  $I_{\text{anode}} = 0.16 A$  and B.C. 1).

83x114mm (300 x 300 DPI)



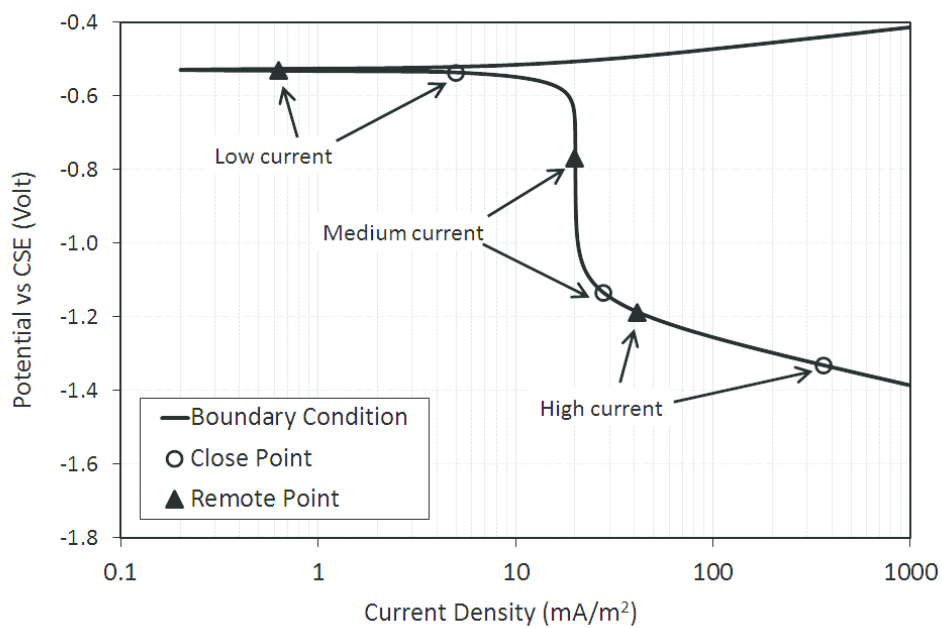


FIGURE 8. Polarization of two points of pipe in different level of applied current.

83x57mm (300 x 300 DPI)

1  
2  
3  
4  
5  
6  
7  
8  
9  
10  
11  
12  
13  
14  
15  
16  
17  
18  
19  
20  
21  
22  
23  
24  
25  
26  
27  
28  
29  
30  
31  
32  
33  
34  
35  
36  
37  
38  
39  
40  
41  
42  
43  
44  
45  
46  
47  
48  
49  
50  
51  
52  
53  
54  
55  
56  
57  
58  
59  
60

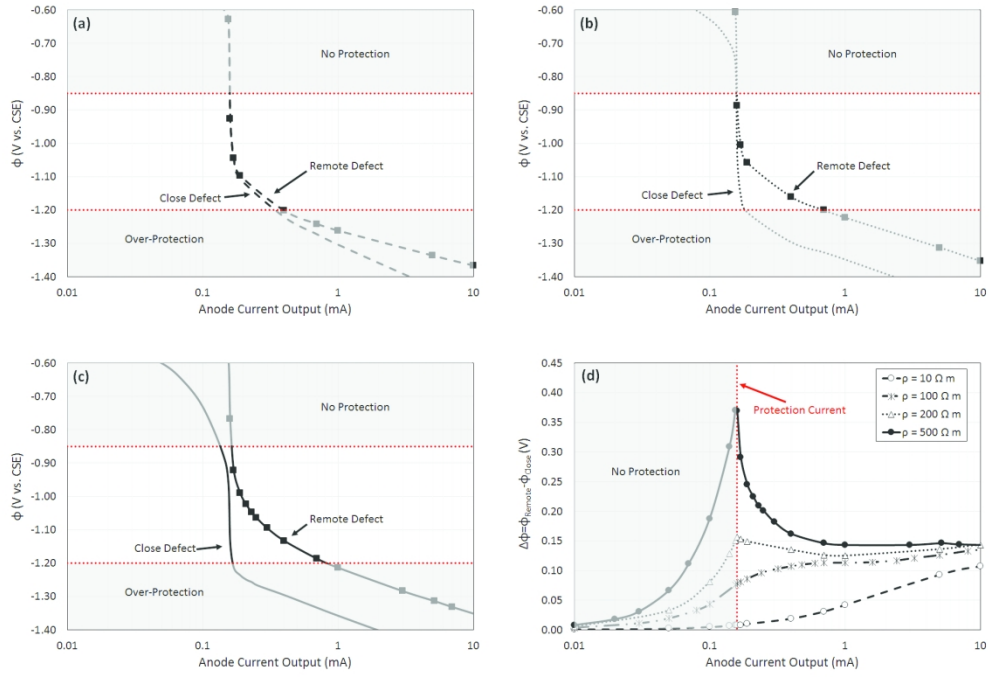


FIGURE 9. Soil resistivity effect in case a (a)  $\rho = 10 \Omega m$ , (b)  $\rho = 100 \Omega m$ , (c)  $\rho = 200 \Omega m$ , and (d) potential difference for presented soil resistivity ( $D_p = 0.4 m$ ,  $r_a = 0.4 m$ ,  $D_c = 1 cm$ ,  $D_R = 10 cm$  and B.C. 1).

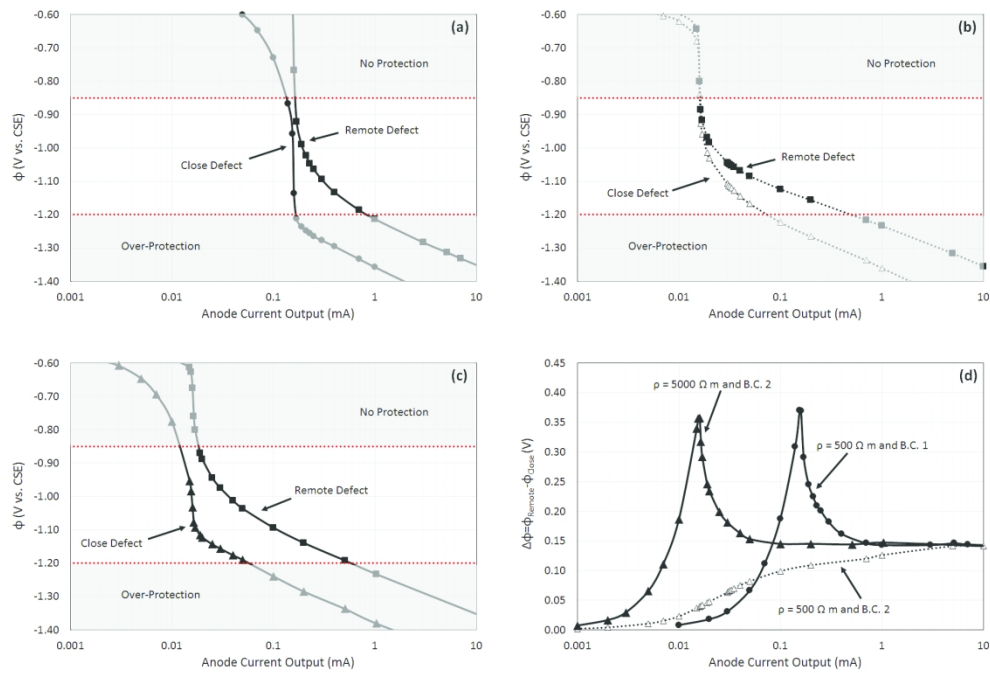


FIGURE 10. Soil resistivity and limiting current density effect in case a (a) B.C. 1 and  $\rho = 500 \Omega \text{ m}$ , (b) B.C. 2 and  $\rho = 500 \Omega \text{ m}$ , (c) B.C. 2 and  $\rho = 5000 \Omega \text{ m}$  (d) potential difference for three mentioned conditions ( $D_p=0.4 \text{ m}$ ,  $r_a=0.4 \text{ m}$ ,  $D_C=1 \text{ cm}$ ,  $D_R=10 \text{ cm}$ ).

1  
2  
3  
4  
5  
6  
7  
8  
9  
10  
11  
12  
13  
14  
15  
16  
17  
18  
19  
20  
21  
22  
23  
24  
25  
26  
27  
28  
29  
30  
31  
32  
33  
34  
35  
36  
37  
38  
39  
40  
41  
42  
43  
44  
45  
46  
47  
48  
49  
50  
51  
52  
53  
54  
55  
56  
57  
58  
59  
60

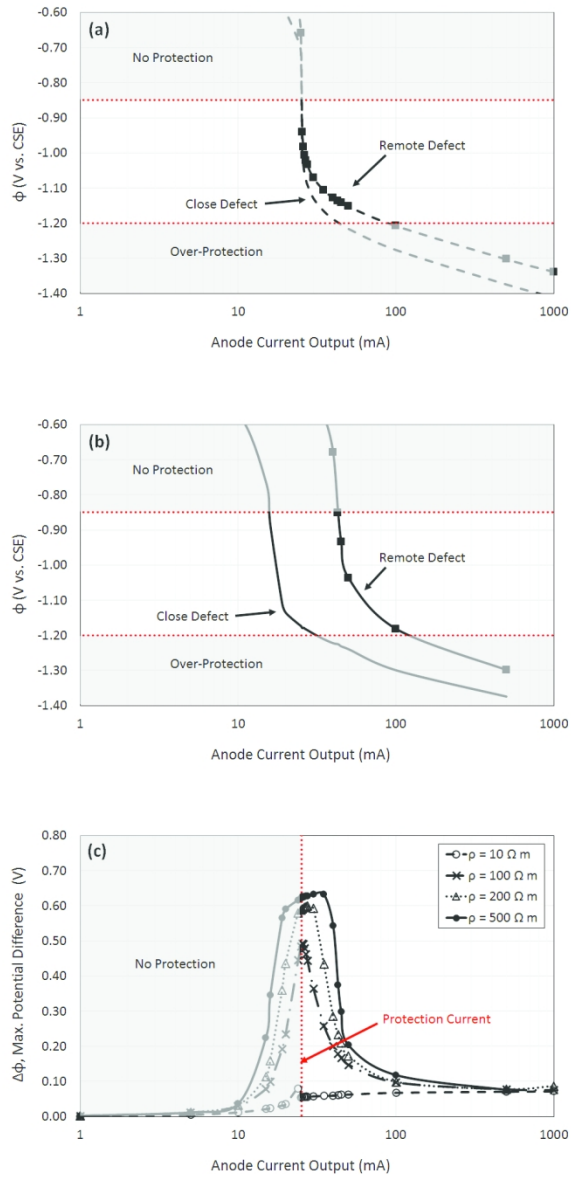


FIGURE 11. Soil resistivity effect in case b (a)  $\rho = 10 \Omega m$ , (b)  $\rho = 500 \Omega m$ , and (c) potential difference for mentioned soil resistivity ( $D_p = 0.4 m$ ,  $r_a = 0.4 m$  and B.C. 1).

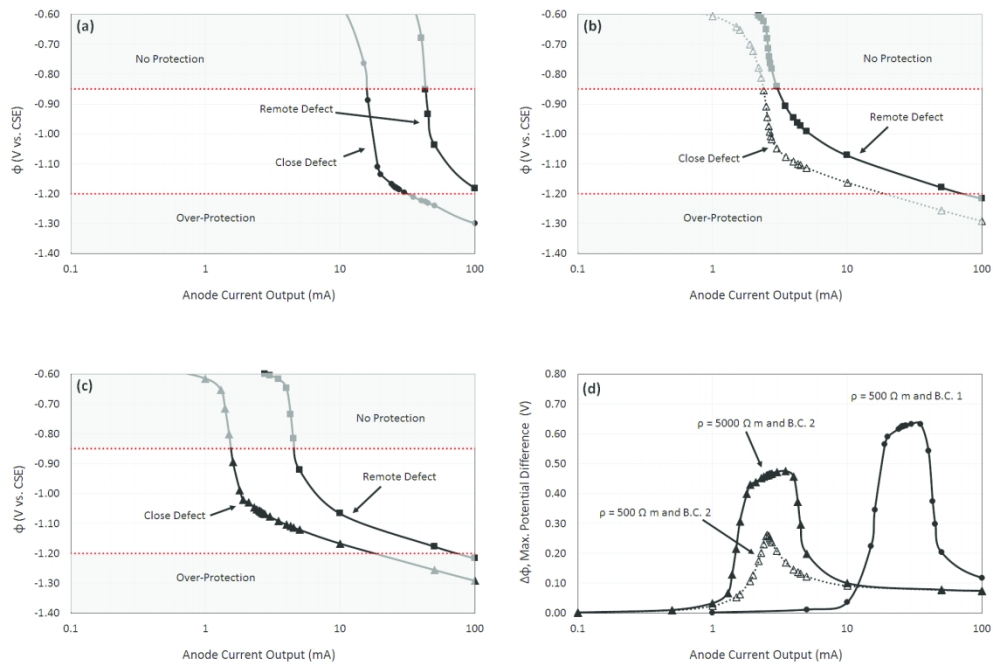


FIGURE 12. Soil resistivity and limiting current density effect in case b (a) B.C. 1 and  $\rho = 500 \Omega \text{ m}$ , (b) B.C. 2 and  $\rho = 500 \Omega \text{ m}$ , (c) B.C. 2 and  $\rho = 5000 \Omega \text{ m}$  (d) potential difference for three mentioned conditions ( $D_p = 0.4 \text{ m}$ ,  $r_a = 0.4 \text{ m}$  and B.C. 1 and 2).

1  
2  
3  
4  
5  
6  
7  
8  
9  
10  
11  
12  
13  
14  
15  
16  
17  
18  
19  
20  
21  
22  
23  
24  
25  
26  
27  
28  
29  
30  
31  
32  
33  
34  
35  
36  
37  
38  
39  
40  
41  
42  
43  
44  
45  
46  
47  
48  
49  
50  
51  
52  
53  
54  
55  
56  
57  
58  
59  
60

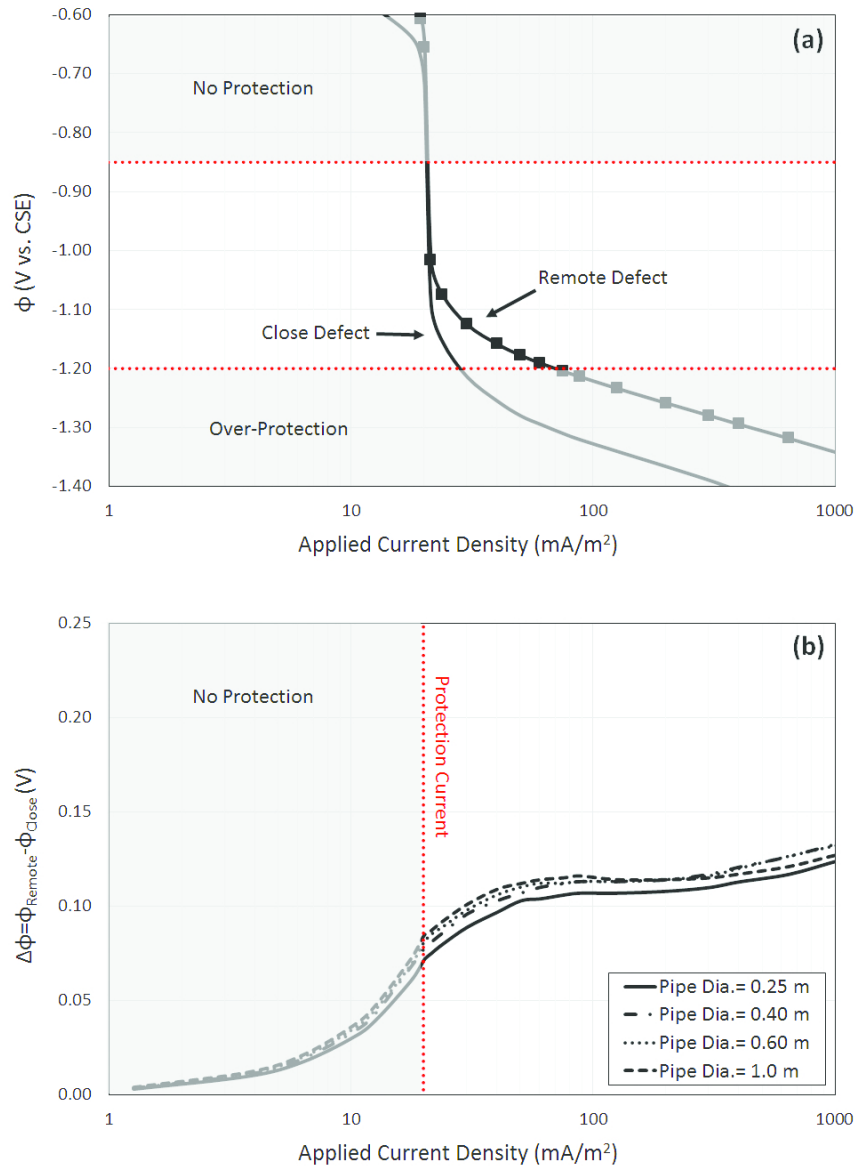


FIGURE 13. Effect of pipe diameter in case a (a)  $D_p = 0.25$  m, and (b) potential difference for mentioned pipe diameter ( $r_a = 0.4$  m,  $\rho = 100 \Omega \text{ m}$ ,  $D_C = 1$  cm,  $D_R = 10$  cm and B.C. 1).

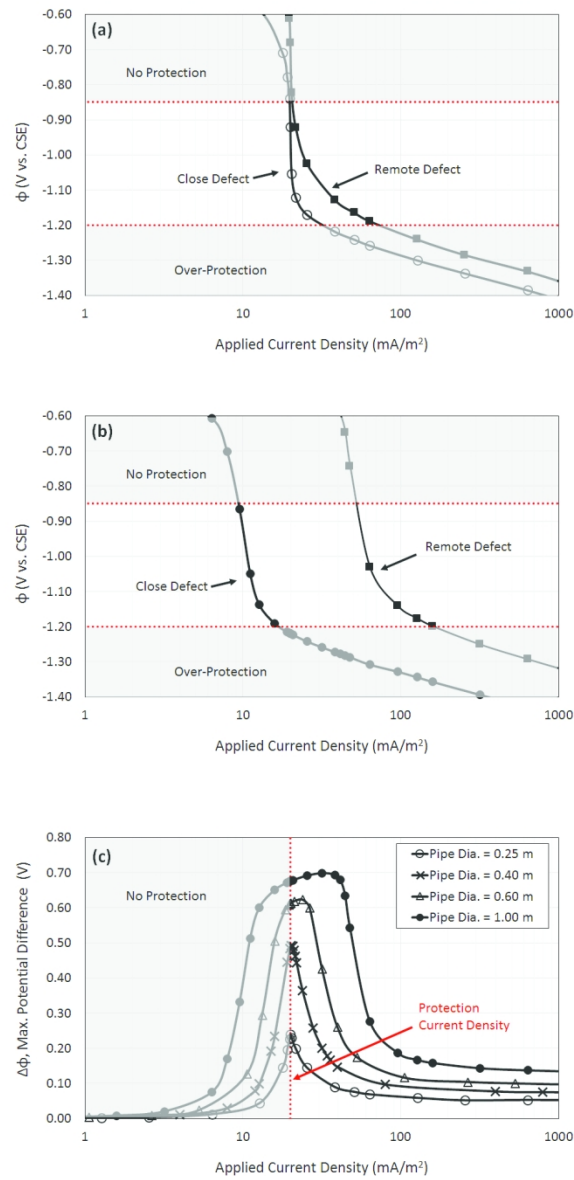


FIGURE 14. Effect of pipe diameter in case b (a)  $D_p = 0.25$  m, (b)  $D_p = 1.00$  m, and (c) potential difference for mentioned pipe diameter ( $r_a = 0.4$  m,  $\rho = 100 \Omega \text{ m}$  and B.C. 1).

1  
2  
3  
4  
5  
6  
7  
8  
9  
10  
11  
12  
13  
14  
15  
16  
17  
18  
19  
20  
21  
22  
23  
24  
25  
26  
27  
28  
29  
30  
31  
32  
33  
34  
35  
36  
37  
38  
39  
40  
41  
42  
43  
44  
45  
46  
47  
48  
49  
50  
51  
52  
53  
54  
55  
56  
57  
58  
59  
60

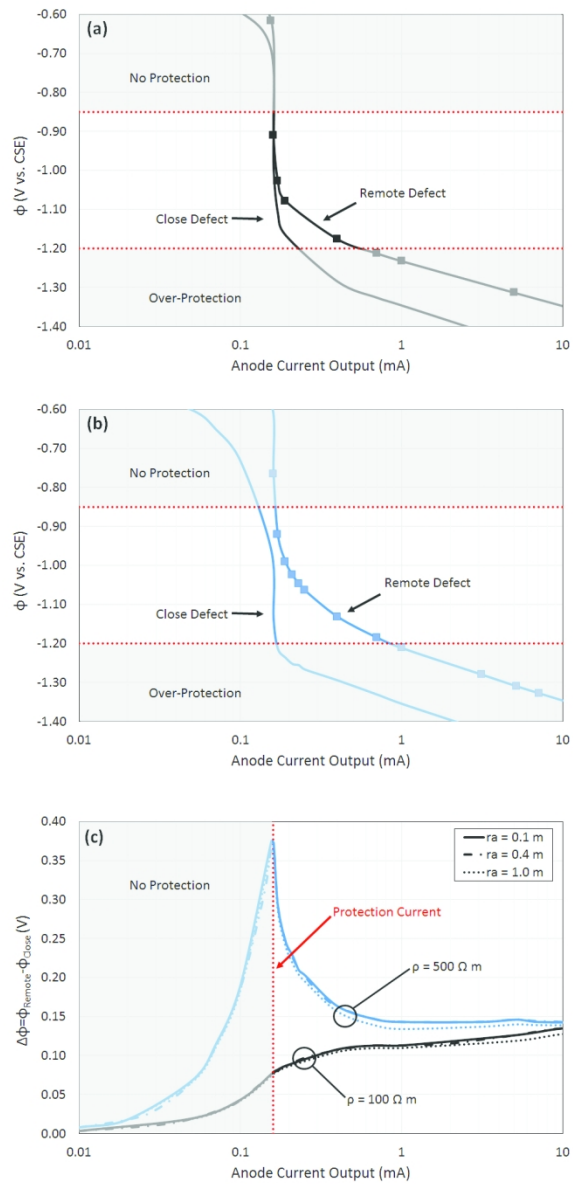


FIGURE 15. Linear anode-pipe distance in case a (a)  $r_a = 0.1$  and  $\rho = 100 \Omega \text{ m}$ , (b)  $r_a = 0.1$  and  $\rho = 500 \Omega \text{ m}$ , and (c) potential difference for two resistivity with different anode-pipe distance ( $D_p = 0.4 \text{ m}$ ,  $D_C = 1 \text{ cm}$  and  $D_R = 10 \text{ cm}$  and B.C. 1).



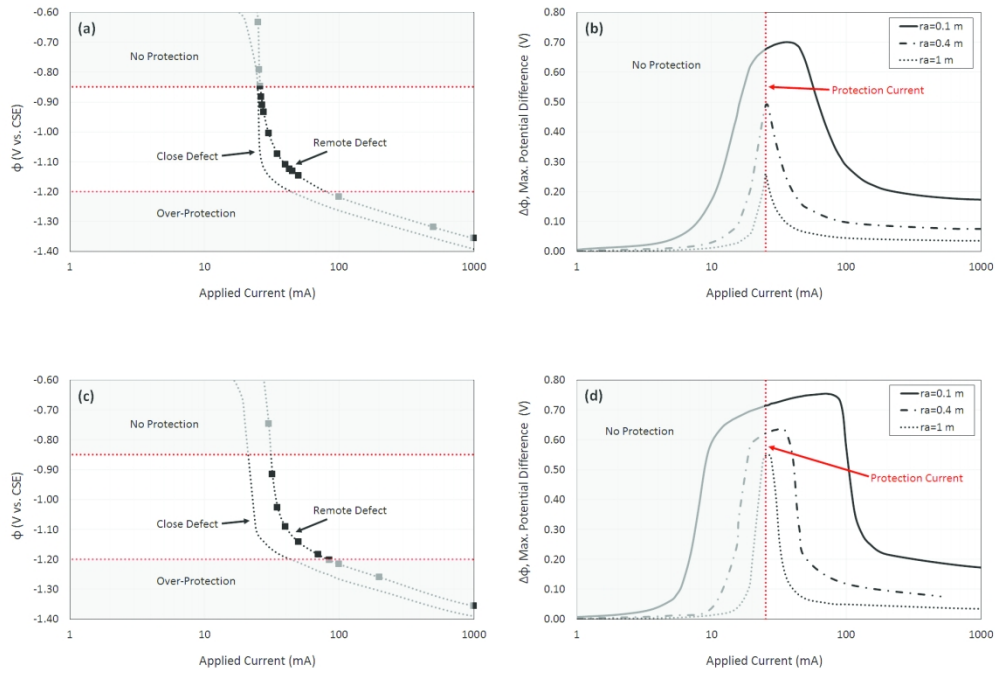
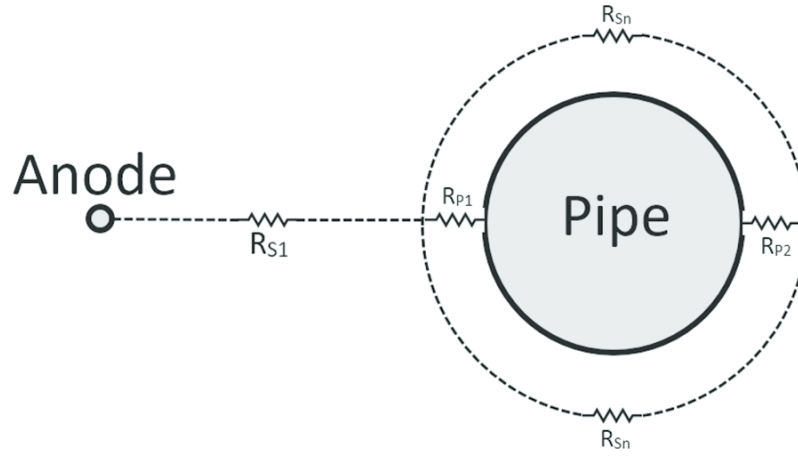


FIGURE 16. Linear anode-pipe distance in case b,  $D_p = 0.4$  m and B.C. 1 for (a)  $r_a = 1.0$  and  $\rho = 100 \Omega m$ , (b) potential difference for  $\rho = 100 \Omega m$  and different anode-pipe distance, (c)  $r_a = 1.0$  and  $\rho = 500 \Omega m$ , and (d) potential difference for  $\rho = 500 \Omega m$  and different anode-pipe distance, (c).

1  
2  
3  
4  
5  
6  
7  
8  
9  
10  
11  
12  
13  
14  
15  
16  
17  
18  
19  
20  
21  
22  
23  
24  
25  
26  
27  
28  
29  
30  
31  
32  
33  
34  
35  
36  
37  
38  
39  
40  
41  
42  
43  
44  
45  
46  
47  
48  
49  
50  
51  
52  
53  
54  
55  
56  
57  
58  
59  
60

(a)



(b)

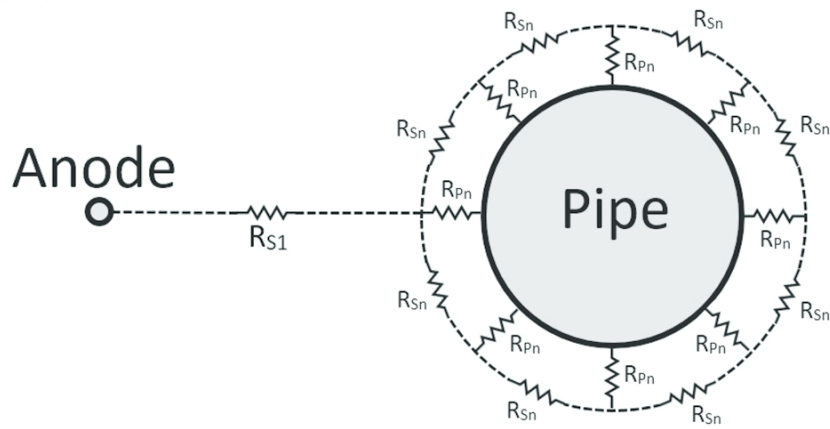


FIGURE 17. Schematic of current paths and proposed resistance for the (a) case a and (b) case b.

83x114mm (300 x 300 DPI)

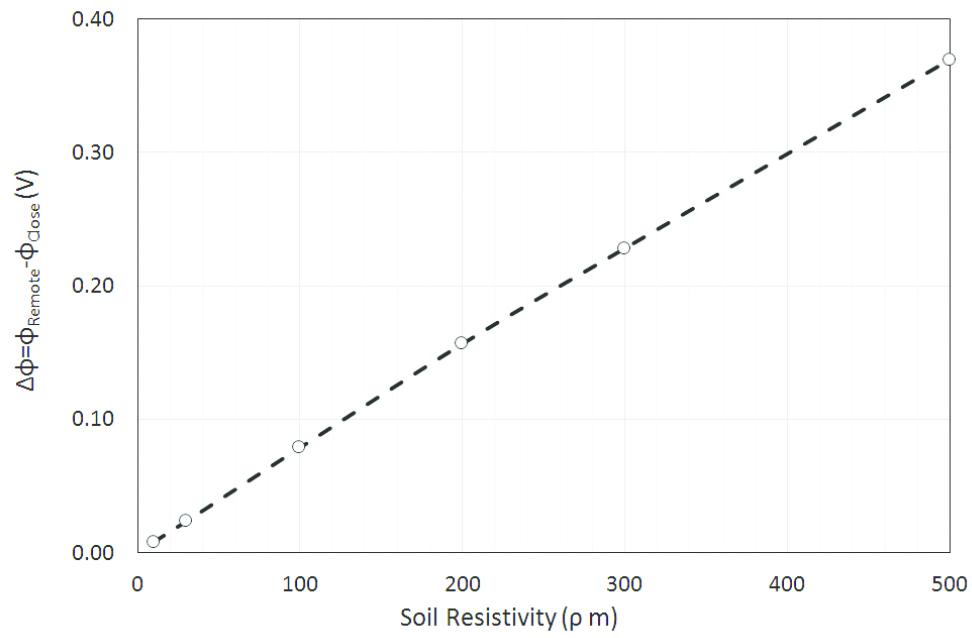


FIGURE 18. Effect of soil resistivity for limited range ( $D_p = 0.4$  m,  $r_a = 0.4$  m,  $D_C = 1$  cm,  $D_R = 10$  cm,  $I_{\text{anode}} = 0.16$  A and B.C. 1).

83x57mm (300 x 300 DPI)